AD-A195 046 A SUBMILLIMETER WAVELENGTH SPACE-BASED IMAGING RADAR 1/1
(U) NAVAL RESEARCH LAB WASHINGTON DC W M MANHEIMER
31 MAY 88 NRL-9111

UNCLASSIFIED F/G 17/9 NL

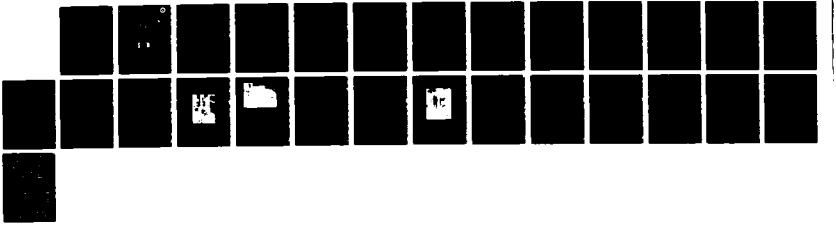

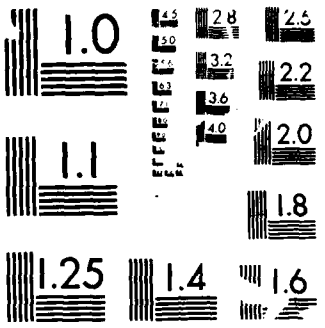

Naval Research Laboratory
Washington, DC 20375-5000

NRL Report 9111

A Submillimeter Wavelength Space-Based Imaging Radar

WALLACE M. MANHEIMER

High Power Electromagnetic Radiation Branch
Plasma Physics Division

May 31, 1988

Approved for public release; distribution unlimited.

SECURITY CLASSIFICATION OF THIS PAGE

REPORT DOCUMENTATION PAGE

Form Approved
OMB No 0704 0188

1a REPORT SECURITY CLASSIFICATION UNCLASSIFIED	1b RESTRICTIVE MARKINGS
2a SECURITY CLASSIFICATION AUTHORITY	3 DISTRIBUTION AVAILABILITY OF REPORT Approved for public release; distribution unlimited.
2b DECLASSIFICATION / DOWNGRADING SCHEDULE	
4 PERFORMING ORGANIZATION REPORT NUMBER(S) NRL Report 9111	5 MONITORING ORGANIZATION REPORT NUMBER(S)
6a NAME OF PERFORMING ORGANIZATION Naval Research Laboratory 6b OFFICE SYMBOL (If applicable) Code 4740	7a NAME OF MONITORING ORGANIZATION
6c ADDRESS (City, State, and ZIP Code) Washington, DC 20375-5000	7b ADDRESS (City, State, and ZIP Code)
8a NAME OF FUNDING / SPONSORING ORGANIZATION Office of Naval Research 8b OFFICE SYMBOL (If applicable)	9 PROCUREMENT INSTRUMENT IDENTIFICATION NUMBER
8c ADDRESS (City, State, and ZIP Code) NRL Accelerated Research Initiative Washington, DC 26375	10 SOURCE OF FUNDING NUMBERS PROGRAM ELEMENT NO: 61153N PROJECT NO: 47-2797-00 TASK NO: RR011-09-4J WORK UNIT ACCESSION NO: DN-157-010

11 TITLE (Include Security Classification)
A Submillimeter Wavelength Space-Based Imaging Radar

12 PERSONAL AUTHOR(S)
Manheimer, Wallace M.

13a TYPE OF REPORT	13b TIME COVERED	14 DATE OF REPORT (Year, Month, Day)	15 PAGE COUNT
Interim	FROM 1/87 TO 1/88	1988 May 31	27

16 SUPPLEMENTARY NOTATION

17 COSATI CODES			18 SUBJECT TERMS (Continue on reverse if necessary and identify by block number)
FIELD	GROUP	SUB-GROUP	Space-based imaging radar; Decoy discrimination; Submillimeter wavelength; SAR and ISAR imaging radar

19 ABSTRACT (Continue on reverse if necessary and identify by block number)

This report considers the use of a submillimeter wavelength space-based imaging radar. The main application envisioned is midcourse decoy discrimination for strategic defense, for which it would have the capability of producing a series of images, in real time, at strategic ranges, with less than meter scale resolution and with modest power requirements. Undoubtedly, there are other applications. The requirements for a SAR and ISAR imaging radar at submillimeter wavelength are determined, and the prospect for the development of rf sources to power the radar is examined.

20 DISTRIBUTION AVAILABILITY OF ABSTRACT	21 ABSTRACT SECURITY CLASSIFICATION
☐ UNCLASSIFIED/UNLIMITED ☐ SAME AS RPT ☐ DTIC USERS	UNCLASSIFIED
22a NAME OF RESPONSIBLE INDIVIDUAL Wallace M. Manheimer	22b TELEPHONE (Include Area Code) (202) 767-3128 22c OFFICE SYMBOL Code 4740

DD Form 1473, JUN 86 Previous editions are obsolete SECURITY CLASSIFICATION OF THIS PAGE

CONTENTS

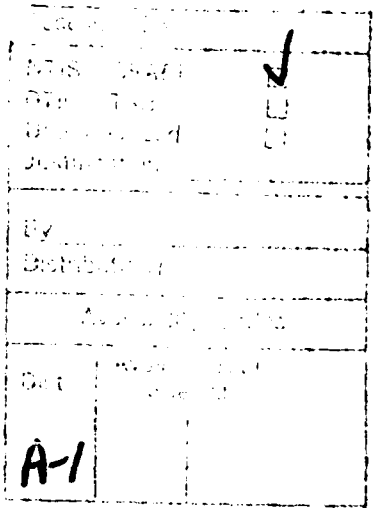

A SUBMILLIMETER WAVELENGTH SPACE-BASED IMAGING RADAR

1.0 INTRODUCTION

This report examines the use of a submillimeter wavelength space-based radar as an asset that can examine objects in space at great range (about 3000 km), in great detail (less than meter scale), and potentially in real time. The short wavelength involved allows for high resolution. For several types of radars, including the synthetic aperture radar (SAR) and inverse synthetic aperture radar (ISAR) that we consider here, the resolution has no explicit dependence on wavelength; when other constraints are included, a very strong implicit dependence favors short wavelength. The radiation sources to power the radar are based on extrapolating low- and moderate-voltage electron-beam-driven sources to the submillimeter wavelength regime. The case will be made that, with modest research and development investment, such sources can be made. The source powers and efficiencies are large enough for the radar applications we propose but are also consistent with space-based use. Furthermore, the cost of microwave tubes is quite reasonable; a SLAC klystron (a microwave tube that operates in the power and voltage range of those we propose here but at a wavelength of 10 cm) and its modulator cost well under $1 million. Such a space-based asset would have many potential applications for both strategic and tactical missions. Our emphasis here is on strategic defense.

Since the problems of target acquisition, decoy discrimination, and kill assessment (SATKA) are some of the most difficult problems in the Strategic Defense Initiative (SDI), and since there is always the possibility that an enemy can interfere with or degrade information transfer, it seems clear that both active and passive devices should operate at many wavelengths. One wavelength range that has received little attention so far is the millimeter to far infrared. This report contends that space-based radars in this frequency range can play a vital role for SATKA.

Potentially many applications exist for such a space-based radar; this report examines the SAR configurations, which would give a series of snapshots in real time of birth-to-death tracking of a target cloud, and the ISAR configuration, which could help decoy discrimination by quickly determining rotation rates of even, smooth spherical targets. ISARs can also use target rotation to generate an image, but here we consider only the simplest ISAR that measures rotation speed.

To realize such radar systems, a variety of new technologies will have to be developed. One, the rf source, is discussed later. These rf sources we discuss are very high power, are fairly efficient (efficiencies of 30% or more with a depressed collector should be achievable), are tunable over a very wide bandwidth, are capable of phase locking and phase control, and in some cases, have wide instantaneous bandwidth. All sources we consider are consistent with space-based operation, although for some, small portions of the spacecraft (< 1 m^3) would have to be pressurized. Next there is the receiver technology. In the submillimeter spectral region, the receiver is a nonlinear element that mixes the received signal with that of a local oscillator (or one of its harmonics) [1]. This mixing creates a difference frequency signal that would be in the megahertz or gigahertz frequency range. Even at very low received power, the mixer is capable of creating a difference frequency signal. The

Manuscript approved February 22, 1988.

returned radar signal may have sufficient power to input directly into the mixing crystal, or may have to be amplified at its original frequency so it has enough power to activate the mixer. In either case, the processing of the returned signal at its original frequency is minimal, or perhaps even nonexistent. The low-frequency signal generated by the mixer is then amplified, and the data processing is accomplished on this lower frequency signal. Thus, regarding the signal and image processing, the more standard techniques used at conventional radar frequencies could also apply to the submillimeter range of the spectrum. In some cases, to generate an image from the returned radar pulse in real time would require enhanced computer capability and could depend on the development of supercomputers.

To focus more clearly on the advantages of the system we propose for SATKA, we now briefly discuss the limitations of other potential systems. First we consider a radar system at a conventional microwave frequency. For any wavelength, the cross range resolution angle of the beam is proportional to the wavelength. Thus, the cross range resolution is about one hundred times better at submillimeter wavelengths than at a more conventional X-band radar. Alternatively, the antenna size can be one hundred times smaller. Typically, space-based microwave radars that operate at strategic range, either space-to-space or space-to-ground, propose antennae many tens of meters or more in size, but smooth to a fraction of a wavelength [2]. For submillimeter wavelengths however, the diameters are meters or less. Although the received power will be smaller by the wavelength squared at given antenna gain, this can be largely overcome in the submillimeter range if the noise level is reduced by cooling the receiver so that the photon energy is larger than the thermal energy. For instance, we will see that the submillimeter wavelength SAR has the potential of operating at average prime powers of under 1 kW, yet providing meter scale resolutions at strategic ranges.

In the spectral region that we are considering, the atmosphere is black so there can be no interference from an Earth based source. Since the radar frequency we consider is high, it is potentially tunable over a wide bandwidth, but it uses only a very narrow bandwidth on each pulse; space-based interference is also very unlikely. Let us focus further on this. If the radar frequency is 10 GHz and 30-cm range resolution is required, the transmit and receive bandwidths must be 1 GHz, or 10% of the total frequency. Thus a jammer does not have to know the frequency very accurately. Now consider a radar at 10^3 GHz. The bandwidth required is still 1 GHz for 30-cm range resolution; however, this is now only 0.1% of the center frequency. Thus a jammer has to know the frequency very accurately. If the radar source has frequency agility, as do those we propose, that jammer must fill the entire band with noise, requiring enormously more power.

We further note that submillimeter radiation can propagate through nuclear debris virtually without interference. An earlier study has shown [3] that for communication from Earth to a geosynchronous satellite, a single, high-altitude nuclear burst can produce strong scintillation over a continent-sized region at X-band for hours after the burst. Even at 60 GHz, strong scintillations are produced over an area many hundreds of kilometers in each direction. Figure 1 shows the regions of strong scintillation 0.5-h after the burst [3]. For horizontal propagation, at an altitude of 1000 km above Earth's surface, the situation is worse. Thus a millimeter to submillimeter wavelength radar has many advantages over conventional microwave radar.

We now consider passive optical systems. The resolution distance for such a system is about $\lambda R/d$, where λ is the wavelength, d is the lens or mirror diameter, and R is the range. For 30-cm resolution at a range of 3×10^3 km and using a wavelength of $\lambda = 5 \times 10^{-5}$ cm, a lens or mirror diameter of 5 m is required. This would be very costly. The Hubble Space Telescope mirror has a diameter of 2.4 m and cost about $5 million [4]. According to the American Physical Society (APS) report [5], the cost of such a mirror is generally proportional to its diameter cubed. Thus such a mirror for an SDI system would cost about $40 million. This is large compared to the cost of the millimeter or submillimeter wave tube.

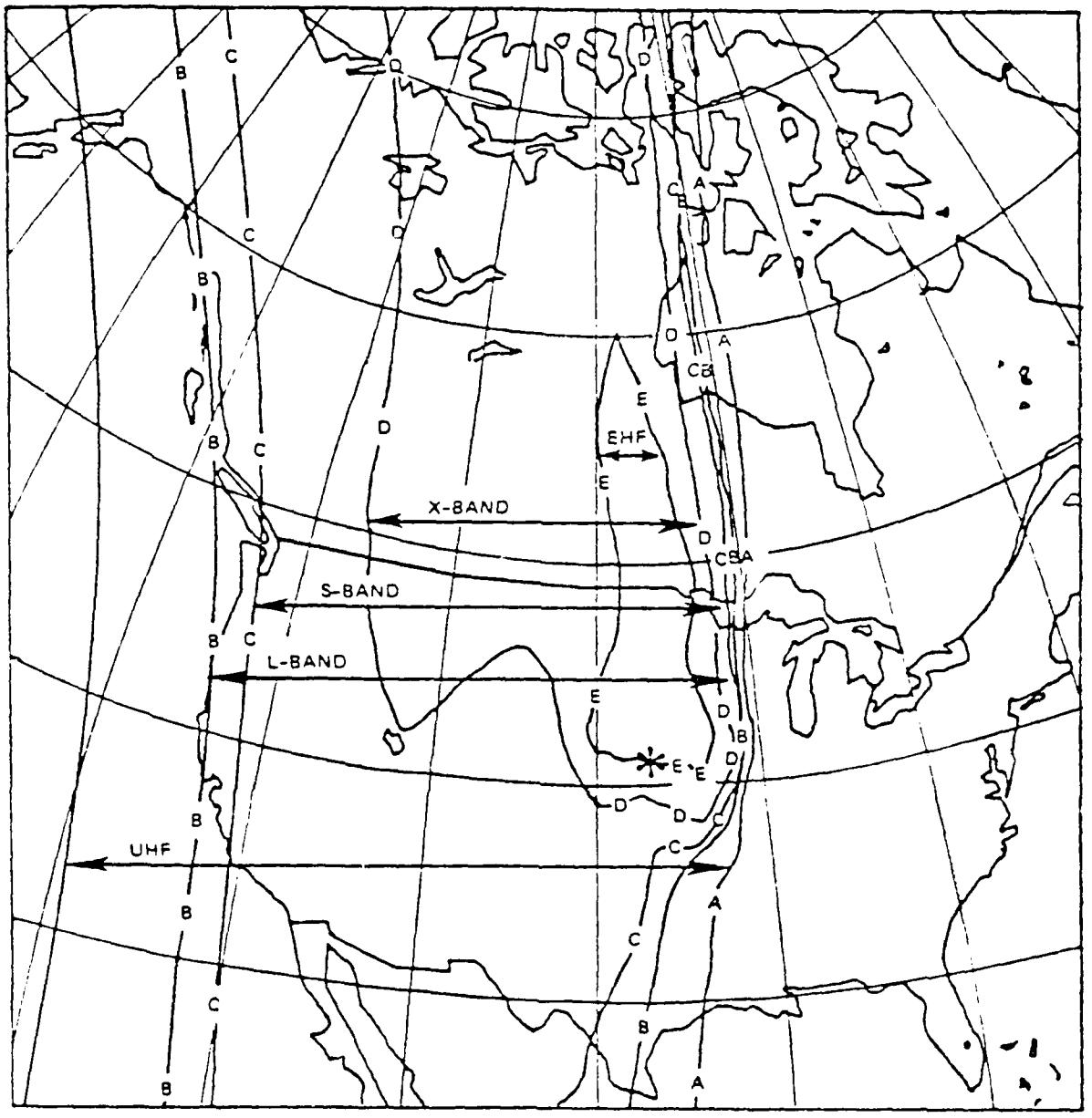

Fig. 1 — Geographical extent of strong scintillation along links between ground and geosynchronous satellite terminals 0.5-h after a high altitude nuclear burst at the star. Note the wide geographic area affected by a single burst, and the strong frequency dependence.

Next, we consider active optical systems. An illuminator that uses angle imaging would have the same size mirror as the passive system. A SAR imaging radar of the type we consider for the submillimeter or microwave radar is possible at optical and IR wavelengths also. Specifically we consider a CO_2 laser-based SAR. Here, reducing the noise level by increasing the photon energy above the thermal energy would not require the same degree of cooling. However, this optical imaging radar has drawbacks. It would have to be powered by a CO_2 laser whose frequency is known to be on one of 50 to 100 specified transition lines between 9 and 11 μm. As we will see, a SAR requires phase coherence over times of tens of microseconds. For a CO_2 laser to achieve this coherence on a particular line, the efficiency is limited to about 5% to 10%. Thus the efficiency is considerably less than the sources we propose here. For a space-based source, efficiency is very important because all

waste energy must be radiated away. At given radiated power, a 5% efficient source must radiate away about eight times more power than a 30% efficient source. Now let us consider the prospect of jamming the CO_2 laser-powered SAR. Because of line-of-sight issues, as well as propagation through the atmosphere, ground-based jamming should be difficult. However, it is not impossible, particularly since there is almost no power limit for a ground-based source. For space-based jamming, a relatively low-power CO_2 laser, which generated noise on many of the available transition lines, would not present a very great weight penalty. We propose that is easier than space-based jamming of the submillimeter wave sources, which will require high voltage and/or high magnetic field just to generate the required frequency. Furthermore, there are effectively thousands of possible lines of operation. Thus a space-based jammer at the submillimeter wavelength would, in all likelihood, present a considerable problem to the offense. Furthermore as we will see, the CO_2 laser radar seems to require about an order of magnitude more radiated energy, and considering the lower efficiency, even more prime power.

2.0 POSSIBLE RADAR CONFIGURATIONS

In this section, we consider two possible space-based radar configurations. Each is a complicated system with many variables. The analyses presented here are meant to sketch possible parameters, and clearly do not represent fully detailed, optimized systems. First, we consider a space-based SAR. This has the potential capability of providing a series of images (about a 1-s time exposure) of all objects in space within a certain region from several hundred meters to several kilometers. This is not a search system therefore, but must be pointed to the approximate spatial region by some other sensor. However, once pointed, it could provide for birth-to-death tracking of all targets and decoys as the reentry vehicles (rv's) and decoys are launched from the main bus. Second, we consider a space-based ISAR. This has the potential capability of very rapidly determining rotation rates of all objects in space by looking at them one at a time. Since only one object should be within the beamwidth for an ISAR, this would be most useful for decoy discrimination later in the midcourse when the decoys have had a chance to separate from one another. As for the SAR, however, another sensor, possibly the SAR, must point the ISAR toward the target or decoy.

The analysis we do here considers the simplest monostatic configuration with the transmitter and receiver at the same place. An alternate bistatic configuration could be used to separate the transmitter and receiver by putting them on two different but nearby satellites. This would be a more complicated system, particularly regarding phase coherence between the two, but it would also make blinding, with corner reflectors, or jamming, much more difficult.

2.1 The Submillimeter Wavelength Space-Based SAR

The imaging schemes that we propose are types of Doppler imaging. The standard use of a SAR is for terrain mapping from satellites and aircraft [6]. Here, the range is resolved by the time delay between the transmitted and (temporally compressed) received pulse. The cross range motion is resolved by the change in Doppler shift. That is, if the beam has angular full width θ, which is equal to $4\,\lambda/\pi d$, where λ is the wavelength and d is the diameter of the antenna, and the cross range velocity of the radar with respect to the object viewed is v, then the Doppler shift of an object at beam center is zero, while the relative Doppler shift of an object at the beam edges is $\pm 2v_\theta/c$. Thus the cross range position of a particular object can be determined from the relative Doppler shift. (Actually, this Doppler shift manifests itself as a phase shift of one part of the received signal with respect to another part, the so-called phase history.) As the radar beam passes over the particular target, its Doppler shift varies over the full range, and a hologram of the target is produced. The image processor then generates an image from the hologram. The important thing to note is that the effective length of the cross range imaging lens is the full radar beam width $R\theta$, where R is the range. Thus

the resolving angle is given by $\lambda/R\theta$, so that the cross range resolution distance works out to be $d/2$, half the antenna diameter. A SAR assumes the target is stationary except for its convection through the beam. If the target is itself moving or spinning, the imaging procedure becomes complicated. Additional imaging procedures might need to be developed, possibly empirically.

We now discuss some simple scaling relations for a space-based millimeter or submillimeter wavelength SAR. The radar range equation relates the received power P_r to the transmitter power P by

$$P_r = \frac{PG^2\sigma\lambda^2}{(4\pi)^3R^4}, \tag{1}$$

where G is the antenna gain and σ is the cross section. By using the relation between the gain and the antenna diameter d (d is the physical diameter only for an ideal radiator; for an actual antenna, d is usually somewhat larger than the physical diameter),

$$G = \pi^2 d^2/\lambda^2, \tag{2}$$

and assuming that the cross sections σ corresponds to the minimum physical area to be resolved $d^2/4$,

$$P_r = \pi d^6 P/256\lambda^2 R^4. \tag{3}$$

This is the received power from a portion of the viewed object corresponding to the minimum resolvable size. This received power must be larger than the noise power, which is

$$P_n = (\Delta f)kT \exp -(hc/\lambda kT), \tag{4}$$

where Δf is the bandwidth of the receiver, k is Boltzman's constant, c is the speed of light, and T is the temperature. The minimum bandwidth of the receiver is that required to resolve the returned radar signal. There are two possible contributions to the bandwidth, the Doppler shift of the target, $2f v_r/c$, where v_r is the component of velocity along the range; and the bandwidth needed to provide the range resolution. We assume that the range resolution is equal to the cross range resolution $d/2$, so that this contribution to Δf is $2c/d$. For meter scale length resolution, and orbital velocities of 10 km/s, the bandwidth required for range resolution is the dominant effect. The noise power can be significantly reduced by cooling the receiver. However, the minimum practical temperature for the receiver is 3 K, the temperature of the background microwave radiation. We assume this temperature, which is a best case value. To achieve it, not only must the receiver be cooled, but the antenna (and its major sidelobes) cannot view the sun or any other bright objects. Furthermore, we assume that the range R is 3000 km, a typical range required for strategic defense. In this case, the signal to noise power depends only on λ, d, and P,

$$P_n/P_r = 1.4 \times 10^8\lambda^2/Pd^7 \exp(4.3/\lambda), \tag{5}$$

where d is in meters, λ is in millimeters, and P is in watts. For operation, we assume the noise to signal ratio must be less than 0.1. This gives a minimum transmitted power for radar operation.

We now consider constraints arising from the fact that the receiver must resolve the phase history emerging from the Doppler shift. The relative Doppler shift is given above. Using it, we find

that the total phase shift from an object at one edge of the beam to an object at the other edge is given by

$$\Delta\phi = 1.6 \times 10^5 \tau/d\,, \tag{6}$$

where τ is the pulse time in seconds, and d is in meters. Also we assume a cross range velocity of 10 km/s. Notice that the phase shift is independent of wavelength. The component of velocity in the direction of the range is proportional to θ which is proportional to λ, while the frequency is proportional to λ^{-1}. To resolve the image, the phase shift from one edge of the beam to the other must be larger than a critical value. If this critical value is less than 2π, a frequency measurement can be made by a single phase measurement rather than by integrating the rate of change of phase shift through the entire returned pulse. We assume the critical phase shift is given by π. This then gives a pulse time for the radiation. We note also that if the total phase shift across the beam is π, the minimum phase resolution to determine a cross range length $d/2$ is given by

$$\pi^2 d^2/8R\lambda. \tag{7}$$

If the receiver is unable to resolve this phase shift, a longer pulse time (and greater total phase shift) would be required for such spatial resolution.

Let us reemphasize here that for the SAR to operate, precise phase information is required for the returned pulse, and conversely, the transmitter must be phase-controlled to a very high degree of accuracy. This underlines the fact that the returned signal should not be degraded by the presence of nuclear debris.

Next we consider the number of photons N the antenna receives from each element of the image during the pulse. It is not difficult to calculate that this is

$$N = 0.75 d^6 P \tau/\lambda. \tag{8}$$

As usual, P is in watts, τ in seconds, d is in meters, and λ is in millimeters. Since coherent processing must be done on the signal, the total number of photons from one element must not be too small. Here we assume that N must be larger than 10. This gives a minimum value of $P\tau$, the energy in each pulse.

Last, we consider several other aspects of the radar system. The length of the time exposure is the time T for the target to cross the full beam width when traveling at a typical orbital velocity, which we assume to be 10 km/s. The field of view F, which is the range times the full angle, relates directly to the number of elements in the image Q since

$$Q = 4F^2/d^2. \tag{9}$$

Finally, there is the maximum pulse repetition rate. If the radar is not to be transmitting when it is receiving, the duty factor should be $< 50\%$. Since we are looking at a target that is assumed isolated, range ambiguity should not be a great constraint as long as the velocity of light times the interpulse spacing is greater than the spatial extent of the target. We assume the pulse rate is 10^3 Hz, but we also assume a minimum of 10 pulses are required to illuminate the target as it moves across the beam. In Table 1, we list as a function of wavelength, parameters for the millimeter and submillimeter wavelength space-based SAR assuming a range of 3000 km, a cross range velocity of 10 km/s,

Table 1 — Parameters of a SAR as a Function of Wavelength for 1 m Resolution (a 2-m dish) Assuming a Temperature of 3 K, a Range of 3000 km, and an Orbital Velocity Across the Beam of 10 km/s

λ (mm)	10	3	1	0.3	0.1	10^{-2} (A)	10^{-2} (B)
P (S/N) (W)	0.75×10^{9}	2.7×10^{7}	1.5×10^{5}	0.6	2.4×10^{-14}		
$\tau(\theta)$ (s)	4×10^{-5}	4×10^{-5}	4×10^{-5}	4×10^{-5}	4×10^{-5}	4×10^{-5}	4×10^{-5}
E (Photon) (J)	2	0.6	0.2	0.06	0.02	2×10^{-3}	2
E (Image) (J)	4×10^{7}	5×10^{5}	10^{3}	3	0.3	2×10^{-2}	20
T (s)	1.5	0.5	0.15	0.05	0.015	1.5×10^{-3}	1.5×10^{-3}
F (km)	15	5	1.5	0.5	0.15	0.015	.5
Q	2.5×10^{8}	2.5×10^{7}	2.5×10^{6}	2.5×10^{5}	2.5×10^{4}	2.15×10^{2}	2.5×10^{5}

and $d = 2$ m (1 m resolution). The transmitter power listed is the minimum for signal-to-noise resolution, the pulse time is the minimum required for phase shift, and the energy is the minimum required for a sufficient number of photons. The other energy value is the minimum required to get one image assuming a repetition rate of 10^3 Hz for the time T (or ten pulses if this is the larger number of pulses). The energy of each pulse is the maximum of the energy required for photons, or the power for signal-to-noise times the time for phase resolution. If the transmitter is 25% efficient, the actual energy generated on the spacecraft to transmit the radiation needed for this image is four times the values given in Table 1. Notice particularly that the entry for a wavelength of 0.3 mm is quite reasonable regarding energy, size of picture, and number of elements in the image. For a 25% efficient source taking one image after another, the average prime p wer is only about 300 W. If only 10 pulses (rather than 50) are used to form the image, the power could be reduced still further (or the temperature requirements could be relaxed).

For comparison, the parameters for two CO_2 laser configurations also are shown in Table 1. Column A shows an extrapolation using a 2-m dish. (We have used 10 pulses to form the image.) All parameters appear reasonable except the last two. Notice that the field of view is only 15 m on a side, and the image is only 250 pixels. Not only is this a very small field of view, but it would be very difficult to keep the object in the field from pulse to pulse. To see this, notice that at 10 km/s orbital velocity, in the round trip time at the speed of light, the object moves 200 m. Once the target is lost, the radar must begin a two-dimensional search in the cross range directions. Column B shows the result for a different CO_2 laser configuration. Here we have considered a different CO_2 laser SAR configuration. We assume that the target is illuminated with a 6-cm antenna, so that the field of view is as for the 300-μm wavelength case. The integration time through the beam, however, is only 1.5 $\times 10^{-3}$ s, (or a cross range distance of 15 m) so the cross range resolution is still 1 m. The receiving optics are now a 2-m dish or lens coupled with a 30-element linear focal plane array. This array is assumed to be oriented to resolve the cross range motions. Thus this CO_2 laser SAR configuration has the same resolution as the 300-μm wavelength case; however, the energy required to form the image is still about an order of magnitude larger. If the CO_2 laser has 10% efficiency, and 20 images

per second are formed as in the 300-μm wavelength case, the prime power would be about 4 kW, more than an order of magnitude higher than for the submillimeter wavelength.

In Table 2, the same quantities are given for $d = 0.3$ m. Notice that the preferable wavelength now shifts down to 0.1 mm. The average power for a 25% efficient source to generate a series of pictures is about 100 kW. This large increase is a result of the strong scaling with d.

Table 2 — As in Table 1, but with 30 cm Resolution (a 60-cm dish)

λ (mm)	10	3	1	0.3	0.1
P (S/N) (W)	2×10^{12}	6×10^{10}	6×10^{8}	2×10^{3}	2×10^{-11}
$\tau(\theta)$ (s)	10^{-5}	10^{-5}	10^{-5}	10^{-5}	10^{-5}
E (Photon) (J)	2×10^{3}	6×10^{2}	2×10^{2}	60	20
E (Image) (J)	10^{11}	10^{9}	3×10^{6}	10^{4}	10^{3}
T (s)	5	1.5	0.5	0.15	0.05
F (km)	50	15	5	1.5	0.5
Q	2.5×10^{10}	2.5×10^{9}	2.5×10^{8}	2.5×10^{7}	2.5×10^{6}

2.2 The Submillimeter Wavelength Space-Based ISAR

The ISAR that we propose here has as its function the use of Doppler imaging to examine rotation rates of different objects in space. For decoy discrimination for SDI, lightweight decoys have different spin and rotation rates than heavier objects. However, if an object is perfectly spherical and is rotating about its center, there will be no Doppler shift from the rotation, and this particular discrimination scheme could not be effective. One advantage of the millimeter and submillimeter wavelength regime is that the inevitable surface roughness on a wavelength scale will always render the object nonspherical for ISAR discrimination.

An ISAR is used differently from a SAR because an ISAR has the beam focused on a single object; two or more objects within the beam will confuse the imaging procedures. Thus an ISAR is more useful later in the midcourse when the decoys have separated from one another. If the distance apart of the different objects to be viewed is given by D, the gain of the antenna must be such that at the range R, the focal spot has an area $< \pi D^2/4$, or

$$G > 4\pi R^2/D^2. \tag{10}$$

For a 1 km separation at a range of 3000 km, $G > 10^8$, so the antenna diameter is related to the wavelength by $d > 3 \times 10^3 \lambda$. The received power, noise power, and number of received photons

are given as in Section 2.1. However, for the SAR, the antenna diameter d was also the resolution distance, whereas for the ISAR, they are specified independently.

The imaging of a rotating object is done by range-Doppler imaging. Consider a linear object rotating end over end about an axis perpendicular to the radar beam. When the object is at a 45° angle to the beam, the closest part has a positive Doppler shift, the farthest part has a negative Doppler shift, and the center has no Doppler shift. For a spherical object rotating about its center, the closest part has no Doppler shift, while the farthest parts contribute a positive Doppler shift on the top and a negative Doppler shift on the bottom.

Let us now consider imaging with meter scale length resolution. For an ISAR, this means range imaging only so that the required bandwidth is $\Delta f = c/r$, where r is the resolution length. The phase shift to be resolved depends on the rotation speed Ω, so that the minimum relative Doppler shift is $2\Omega r/c$. This corresponds to a minimum phase shift given by

$$\Delta\phi = 4\pi \times 10^3 \Omega r \tau/\lambda. \tag{11}$$

The factor of 10^3 is because r is in meters, while λ is in millimeters. The pulse time τ is determined so that the minimum phase shift is above some critical value. For the 1-m resolution at a range of 3000 km, an antenna gain of 10^8, and a receiver temperature of 3 K, the noise-to-signal power ratio is given by

$$P_n/P_r = 1.9 \times 10^5/\lambda^2 P \exp(4.3/\lambda). \tag{12}$$

The number of photons received is now given by

$$N = 3 \times 10^2 \lambda^3 P \tau. \tag{13}$$

As in the previous subsection, λ is in millimeters, r is in meters, τ is in seconds, and P is in watts. As with the SAR, these formulas give a minimum power for signal-to-noise ratio, a minimum pulse time τ for phase detection, and a minimum total pulse energy to receive enough photons. Table 3 shows the parameters of the ISAR assuming a signal-to-noise ratio of 10, a minimum rotation velocity of 3 m/s ($= r\Omega$), a minimum phase shift of $\pi/6$, and 10 photons for coherent signal processing. Note that for long wavelengths, the pulse energy is determined by the minimum power-to-exceed noise times the minimum pulse time for phase resolution, whereas for short wavelength, the pulse energy is determined by the need to have sufficient photons. Notice also that the parameters of this particular ISAR configuration are much more modest than those for the SAR because the SAR images one entire region of space with everything in it in two dimensions, while the ISAR just takes a single shot of one object. This single shot provides a much smaller field of view than was the case for the SAR. For the ISAR, the minimum pulse energy for the parameters of Table 3, is at a wavelength of 1 mm. However, the smaller antenna required at $\lambda = 0.3$ mm might be worth the added penalty in average power.

The ISAR would have to take many single shot images of targets in space, and would undoubtedly have to take more than one image of a particular object. Since the beam would have to move around a great deal, the antenna would have to be a phased array. Thus in addition to the phase information required for the signal processing, the source must be phase locked in order that the power can be radiated through a phased array. The same comments regarding propagation through nuclear debris made for the SAR also apply to the ISAR.

Table 3 — Parameters for an ISAR as a Function of Wavelength
Assuming a Temperature of 3 K,
a Range of 3000 km, and Meter-Scale Length Resolution

λ (mm)	10	3	1	0.3	0.1
P (S/N) (W)	10^4	5×10^3	3×10^3	10	4×10^{-11}
$\tau(\theta)$ (s)	3×10^{-5}	10^{-5}	3×10^{-6}	10^{-6}	3×10^{-7}
E (Phot) (J)	3×10^{-5}	10^{-3}	3×10^{-2}	1	30
d (m)	30	10	3	1	0.3

3.0 RF SOURCES FOR THE SPACE-BASED RADAR

In recent years, great progress has been made in the development of powerful, efficient rf sources in the millimeter and, to a lesser extent, the submillimeter wavelength region of the spectrum. The fact that the source must be consistent with space-based operation puts many constraints on it. Two powerful millimeter and submillimeter sources are the free electron lasers at Lawrence Livermore National Laboratory [7], and at University of California at Santa Barbara [8]. The former is driven by an induction LINAC at a voltage of 3.5 MeV, and the latter is driven by an electrostatic accelerator, also in the same voltage range. Neither source, as currently configured, is consistent with space-based operation. Not only is the voltage too high, but the size and weight of the sources are also too great for space-based operation. Furthermore, the efficiency of the beam generation schemes themselves must be high in a space-based application, because the efficiency is directly related to the waste heat that must be radiated away. For these reasons, we consider here only electron beam sources based on conventional modulators. These conventional modulators are relatively compact, and they are by far the most efficient generators of electron beams. Thus, a great premium on working with voltages is consistent with these modulators, i.e., a voltage below 500 kV to 1 MeV.

At the high voltages of these conventional modulators, a concern exists about space-based operation. In the space environment, these voltages could cause breakdown and arcing unless the system is pressurized. However, when operating at the half megavolt to megavolt level, it is important to realize that the main energy store is at a much lower voltage, typically about 40 kV. Only for a very short time, and in a very localized position is the full voltage ever realized. For instance, if the final voltage is less than 750 kV, the current less than 200 A, and the pulse time less that 50 μs, a transformer system should be able to generate a pulse with about 0.5 m^3 being pressurized. Once the voltage gets to the megavolt region, a Marx generator would be necessary, requiring a larger pressurized region. While there is concern about high voltage for conventional modulator driven systems, the voltages are much less than those required with alternate schemes to produce high-power submillimeter wavelength radiation.

With a conventional modulator driven space-based source, the idea is to restrict the voltages to below a megavolt and to push every other parameter to the limit. For instance, with a gyrotron or

cyclotron autoresonance maser (CARM) system, large magnetic fields and/or harmonic operation might be required; for a free electron laser (FEL) system, a small period wiggler would be required. Currently there are a number of experimental programs on high-voltage modulator-driven sources at the Naval Research Laboratory (NRL), Massachusetts Institute of Technology (MIT), the University of Maryland (U of Md), and the University of California (Los Angeles) (UCLA). The size of the NRL long-pulse CARM experiment compared to other accelerator based experiments is shown in Fig. 2.

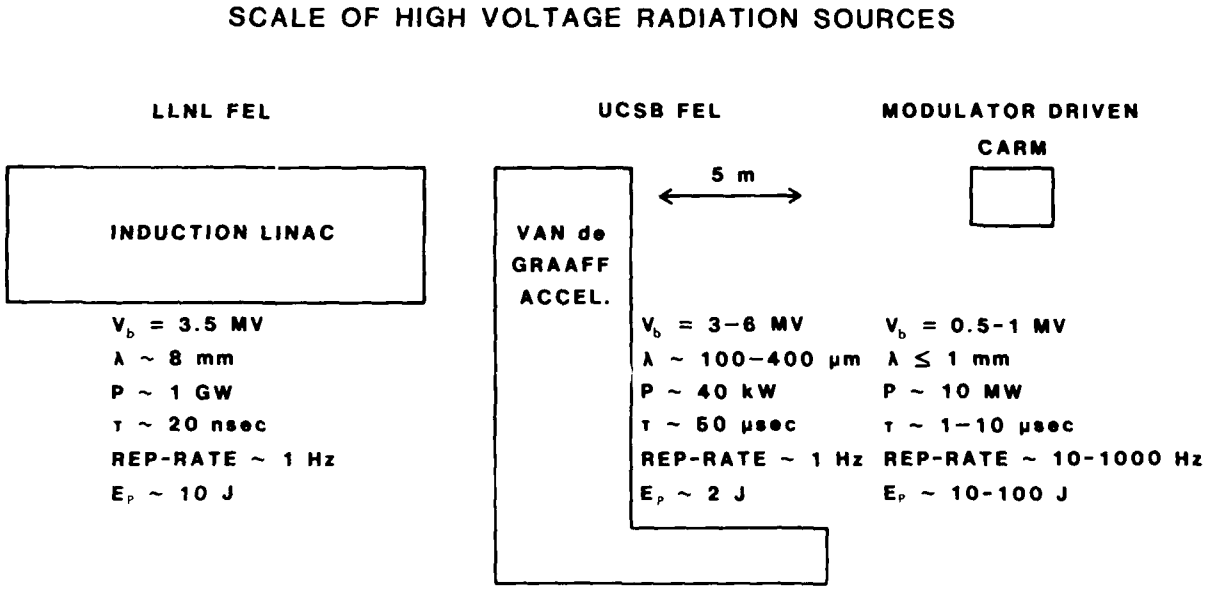

Fig. 2 — Relative sizes of a conventional modulator driven system compared to one driven by an electrostatic accelerator or an induction LINAC

Consistent with space-based operation, many modern rf source concepts have evolved in recent years. With further development, these could power submillimeter wavelength space-based radars. These include the gyrotron, the quasi-optical gyrotron, the CARM, and the small period wiggler FEL. Recent developments in these sources are now discussed. All of these devices are characterized as fast wave devices. This means that all such devices operate without resonant slow-wave periodic structures. In a slow-wave device, the periodicity length of the structure is usually less than a wavelength, and the fields fall off from the structure in a distance of order the periodicity length divided by 2π. Thus as the wavelength gets smaller, the power handling capability also gets worse. A scaling law $P \sim \lambda^{5/2}$ is often invoked for slow wave devices. Fast wave devices, on the other hand, operate under no such constraints; the size of the device is usually determined only by mode competition, and at comparable wavelengths, have much greater size and therefore power handling capability. This advantage particularly comes at the millimeter and submillimeter wavelengths. Figure 3 shows schematics of three different fast wave devices—the gyrotron, the CARM, and the FEL.

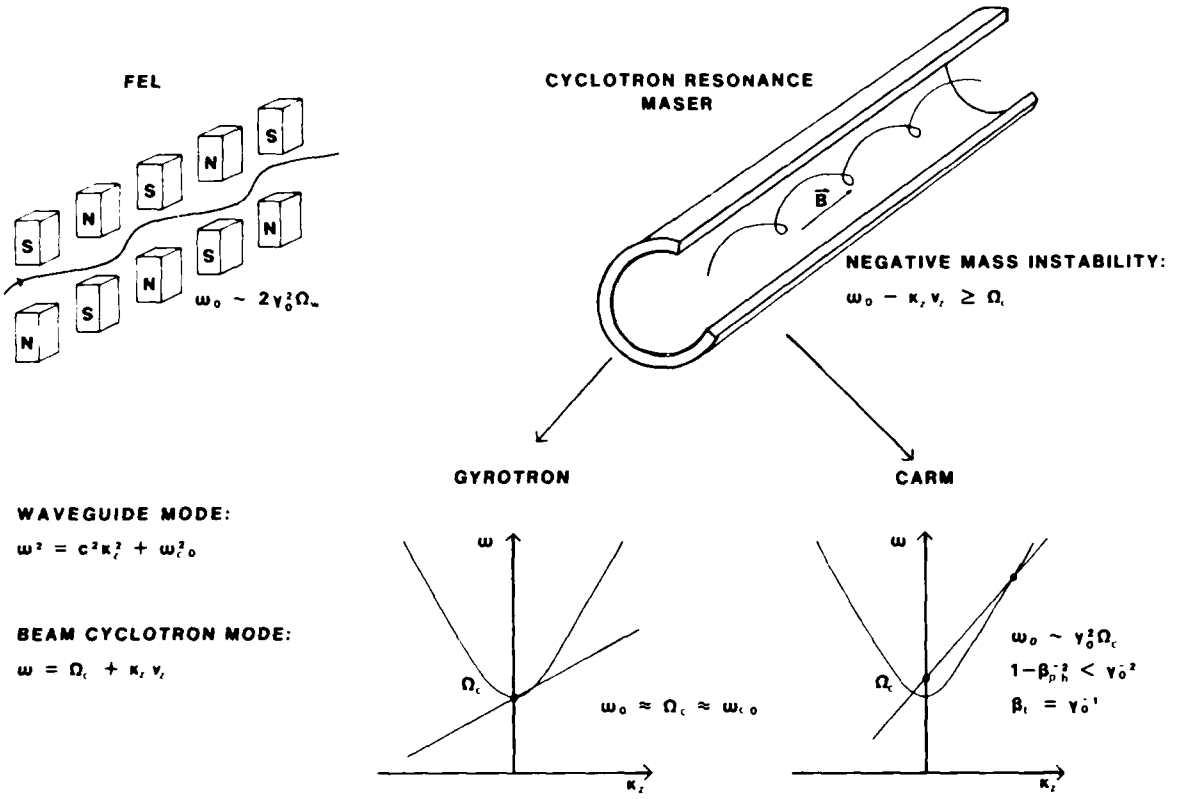

Fig. 3 — The FEL, gyrotron, and CARM

3.1 Cavity Gyrotrons

In a cavity gyrotron, an electron beam with transverse energy (Larmor motion) passes through a cavity near the cutoff. Here the magnetic field is parallel to the axis of the cavity; thus the wave propagation is mainly perpendicular to the magnetic field. As the beam traverses the cavity, it loses part of its transverse energy to the radiated fields if the frequency is roughly equal to both the cyclotron frequency and the cutoff frequency of the cavity. To operate at high frequency, a large magnetic field is required, and this comes from a superconducting magnet. Currently, the highest fields available are about 150 kG from NbSn superconductors, although the field of superconductivity is evolving rapidly at this time. If the magnetic field is denoted B, the wavelength of the radiation is given by

$$\lambda(\text{mm}) = 100/B(kG)n \,, \tag{14}$$

where n is the harmonic number. Because of the relativistic decrease in cyclotron frequency with electron energy, gyrotrons achieve highest frequency at low voltage. This constitutes a particular advantage of gyrotrons for space-based operation. Operation at the fundamental can be at submillimeter wavelength for the maximum field of 150 kG. Shorter wavelengths can be generated by operating the harmonics.

Gyrotrons were initially developed in the Soviet Union, and the Soviets are still very active in this field. Generally, they have achieved more than the West [9]. Gyrotrons have demonstrated very

high power capability at millimeter wavelengths. For instance, the gyrotrons developed at MIT have demonstrated powers of roughly 0.5 MW at efficiencies up to 25% in a frequency range from 140 to 250 GHz. The tunability is achieved by varying the magnetic field and tuning from one cavity resonance to another in first a series of TE_{m2} modes, then a series of TE_{m3} modes, and finally, a series of TE_{m4} modes [10]. This gyrotron used a thermionic beam consistent with long pulse, or cw operation. Another series of experiments at MIT yielded operation at the second harmonic at submillimeter wavelength, although at much lower power and efficiency [11]. Figure 4 shows the MIT gyrotron.

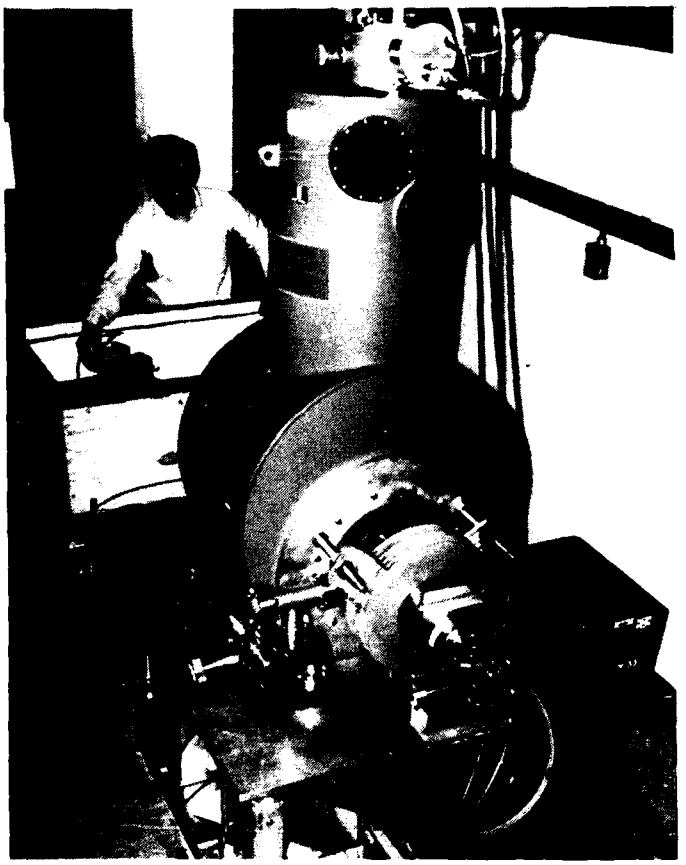

Fig. 4 — The MIT gyrotron

A similar series of experiments took place at NRL but used a higher voltage beam produced by a compact febetron pulse line accelerator. In these experiments, beam voltage was typically 750 kV, beam current was 1 to 2 kA and the pulse time was about 20 ns. Other febetron modules of the same size have pulse lengths >200 ns. Figure 5 shows the febetron gyrotron experiment. The febetron pulser is the cylinder behind the pancake magnets. As is apparent, the febetron is compact, perhaps more compact than a conventional modulator. However, the quality of the voltage pulse is much poorer, and the maximum pulse time is much less. In these experiments, up to 100 MW of power at efficiencies of up to 10% were produced at frequencies ranging from 25 to 50 GHz. As in the MIT experiments, tunability was achieved by tuning the magnetic field through a series of TE_{m2} modes. In both the NRL and MIT experiments, by properly placing the position of the electron beam in the cavity, it was possible to select a particular cavity mode from a very dense spectrum [12].

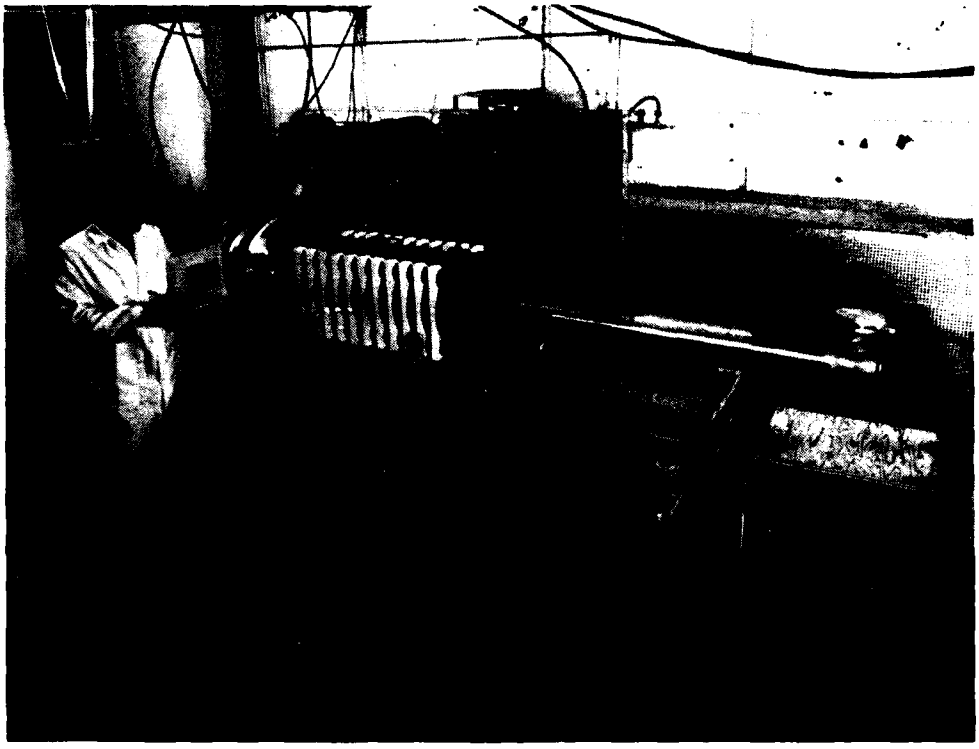

Fig. 5 — The NRL febetron gyrotron

As is pointed out in the discussion of the radar applications, not only is power very important, but very precise frequency control is also crucial. It might be thought that this would require an amplifier rather than an oscillator. An amplifier might be the preferred choice if it were just as easy to develop. However, experience has shown that amplifiers are much more difficult to develop for long pulse, highly overmoded systems. An alternate strategy would be to develop a phase-locked oscillator. At high power, there appear to be two methods to phase lock an oscillator. First, one could use direct injection of a low-power signal through a circulator into the gyrotron cavity in an attempt to phase lock a much higher power oscillator. Direct-injection locking of a gyrotron has worked at 35 GHz by using a TE_{01} mode gyrotron oscillator locked by a magnetron [13]. It has been shown that the gyrotron can be locked with injection power 30 dB down from the oscillator power, and that the locking condition obeys Adlers relation. An alternate scheme to phase lock the gyrotron is to prebunch the beam in a separate prebunching cavity. An experiment on phase locking by a prebunching cavity was performed at NRL on a fundamental mode gyrotron operating at 4.5 GHz [14]. The use of prebunching cavities was shown to significantly increase the locking bandwidth. Another experiment to test phase locking by prebunching is under construction at NRL [15]. This experiment will investigate phase locking at high frequency with an overmoded gyrotron oscillator. The gyrotron will operate at 85 GHz in a TE_{13} mode ~ 100 kW. Figure 6 shows a schematic of this phase-locked oscillator experiment.

For the bandwidth of the phase locked oscillators, one starts with Adlers relation

$$\frac{\Delta f}{f} = \frac{1}{2Q}\left(\frac{P_L}{P}\right)^{1/2}, \tag{15}$$

PHASE-LOCKED GYROKLYSTRON OSCILLATOR

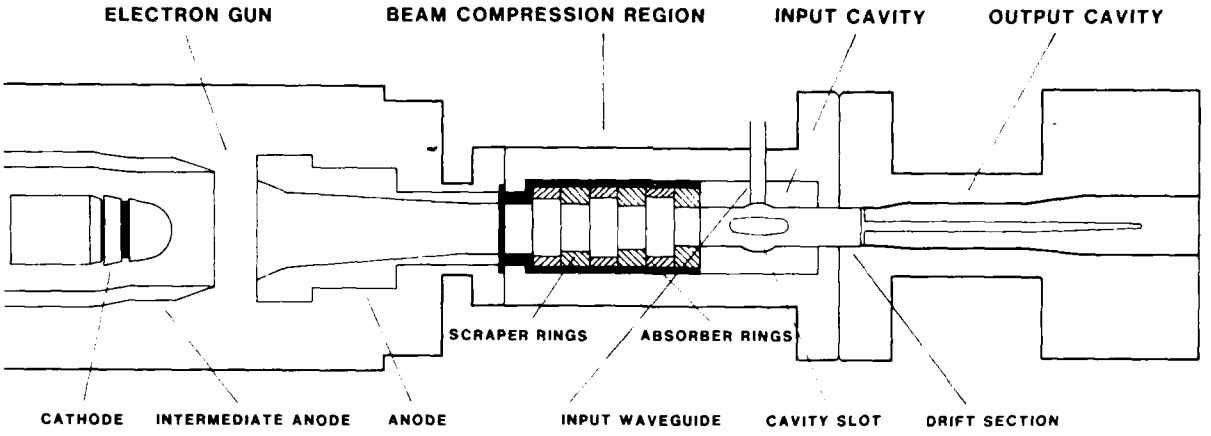

Fig. 6 — The NRL 85 GHz phase locked oscillator

where Q is the quality factor of the cavity, P_L is the locking power, and P is the oscillator power. For typical gyrotron cavities, this gives a relative frequency bandwidth of between about 10^{-4} to 10^{-3}. Use of prebunching cavities could increase the bandwidth considerably. The bandwidth required is generally that for range resolutions, $\Delta f \approx c/d$, so for meter resolution, the bandwidth required is about 300 MHz. Thus, submillimeter phase locked gyrotrons should be able to provide the bandwidth necessary for range resolution.

3.2 Quasi-Optical Gyrotrons

At some frequency, microwave techniques will be less effective, and optical techniques should take over. One attempt to join gyrotrons and optical techniques is the quasi-optical gyrotron [16]. Here the cavity is an optical cavity formed by two spherical mirrors. A magnetic field is transverse to the axis of the cavity, and an electron beam with transverse energy (similar to a gyrotron beam) propagates along the magnetic field. The actual beam wave interaction is the same as in a cavity gyrotron; however, the output radiation is taken at the mirrors. In the quasi-optical gyrotron, the transverse mode structure is identical for all modes, so the output coupler will be nearly independent of frequency. Also, there is a natural separation between electron beam and radiation, and this makes the use of a depressed collector straightforward. Furthermore, since the mirrors are adjustable in space by micrometers placed outside of the vacuum system, one can easily adjust the cavity to have a particular value of Q, resonant frequency, or mode spacing.

An initial experiment on the quasi-optical gyrotron has been performed at NRL [17,18]. Figure 7 shows a schematic of the experiment, and Fig. 8 shows the actual experiment. Notice that the quasi-optical gyrotron requires the use of a superconducting magnet with two radial access ports. These experiments have shown that power up to 80 kW could be generated with efficiencies in excess of 10%. The resonant frequency was easily tunable between 100 and 120 GHz by magnetic field. As the magnetic field varied, the mode jumped between a series of TEM_{00} cavity modes having a different longitudinal mode number.

More recent experiments have shown that in some circumstances, the quasi-optical gyrotron produced power at the cyclotron harmonic [18]. One particular advantage of the quasi-optical gyrotron is that optical techniques could be used to select a higher harmonic over a lower harmonic. For

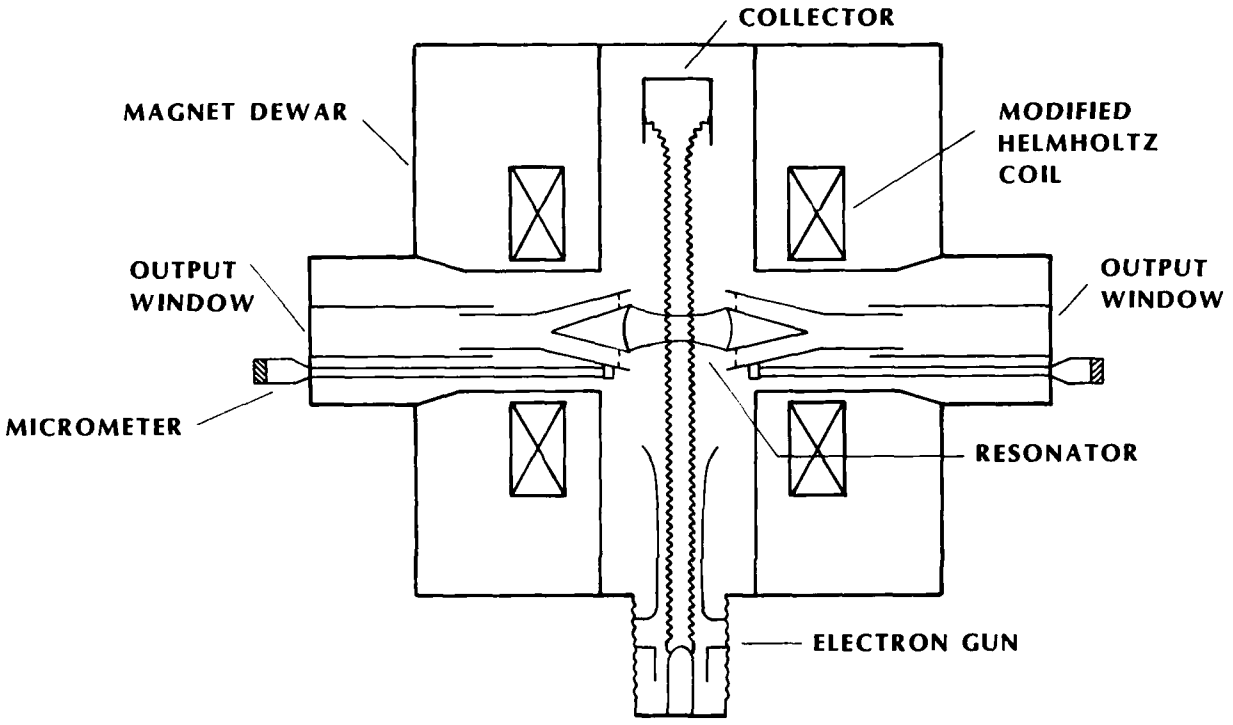

Fig. 7 — The NRL quasi-optical gyrotron

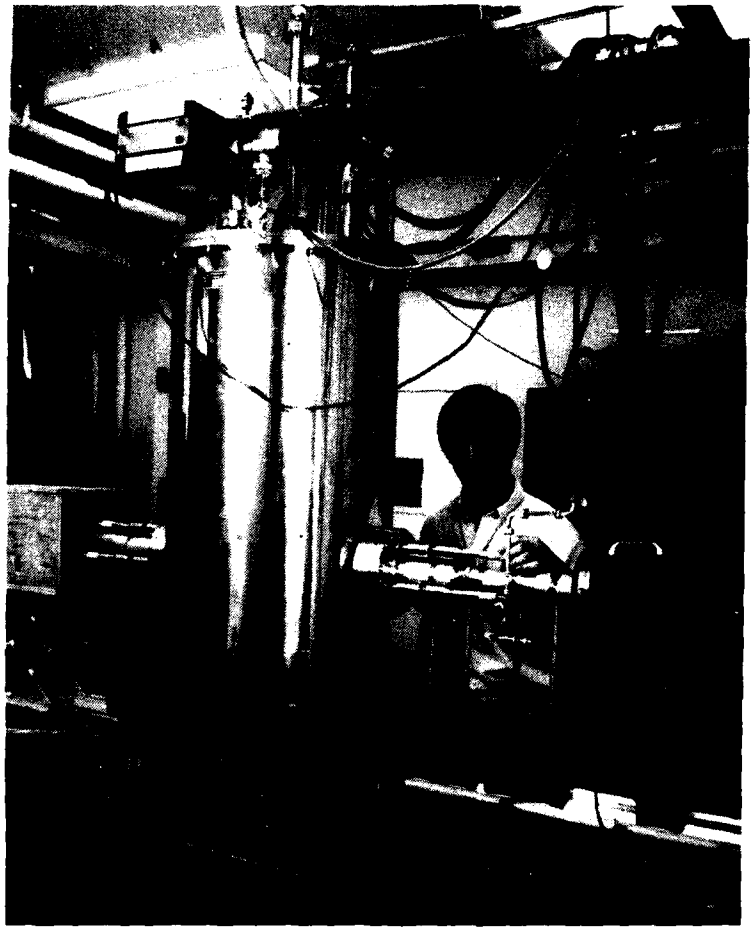

Fig. 8 — The quasi-optical gyrotron

instance, the mirror size could be reduced to better confine the narrower radiation beam at the harmonic [19]. This technique has been shown theoretically to work up to the eighth harmonic, albeit with low efficiency [20]. Furthermore, other optical techniques such as a grating in place of one or both of the mirrors could select higher harmonics over the lower ones.

The NRL quasi-optical gyrotron uses the heterodyne techniques mentioned in the Introduction to measure the frequency. The MIT experiment also uses similar techniques. Here a voltage-tuned local oscillator produces power (milliwatts) from 12 to 18 GHz. This and the signal from the gyrotron are mixed in a mixing crystal. The gyrotron signal and some harmonic of the local oscillator are mixed to a low frequency and put through a band pass filter so that the frequency is determined to very high accuracy. Figure 9 shows a schematic of the heterodyne system. The quasi-optical gyrotron so far has a free-running oscillator only. To phase lock it, one could use a prebunching cavity as in the case of a conventional gyrotron [21].

3.3 Cyclotron Autoresonance Masers

Figure 3 shows the CARM operating as a Doppler shifted gyrotron on the upper intersection of the beam waveguide dispersion relation. Experimental work on CARMs has been done only in the Soviet Union [22] although a great deal of theoretical work has been done in the United States [23,24]. The Soviet experiments have used pulseline accelerators and have generated power at 2 to 4 mm wavelengths with about 3% efficiency. Although the exact frequency of the CARM depends on details of the beam wave interaction, a rule of thumb is that the wavelength is given by

$$\lambda(\text{mm}) = 100/B(kG)\gamma n \,, \tag{16}$$

where γ is the relativistic factor

$$\gamma = E/mc^2 \,, \tag{17}$$

E being the electron energy. Thus with moderate voltages and fields, one can achieve a very short wavelength. For instance, a 150 kG field with a 500 kV beam could generate 300 μm wavelength radiation. Operating at the second harmonic would reduce the wavelength by an additional factor of two. However, the CARM does demand a very high quality electron beam with very little spread in longitudinal velocity. Designing the electron gun is one of the greatest challenges of CARM research. Finally, the CARM, unlike the cavity gyrotron when run as an amplifier, should have wide instantaneous bandwidth.

Although no CARM experiments are in the West yet, four are in advanced planning stages. One is a CARM oscillator at 100 GHz driven by a pulse line accelerator at NRL [25]. The beam voltage is is about 1 MV, the current about 200 A, and the pulse time is about 50 ns. The electron gun is a cold cathode gun, but one that uses focusing electrodes made of anodized aluminum, which hold off electron emission. This experiment will operate in a TE_{61} mode, will use a Bragg resonator to provide longitudinal mode selectivity, and is designed to generate 10 to 20 MV at about 10% efficiency. Figure 10 shows a schematic of this experiment. Another CARM experiment is being designed at MIT. It is a 140 GHz amplifier driven by a thermionic beam with a voltage of 750 kV and a current of about 50 A. This experiment is an amplifier operating in either the TE_{11} or TE_{21} mode and is designed to generate a power of 10 MW [26]. Two other CARM experiments in the very early design phases are the 560 GHz CARM amplifier at UCLA [27], and the 250 GHz CARM oscillator at NRL.

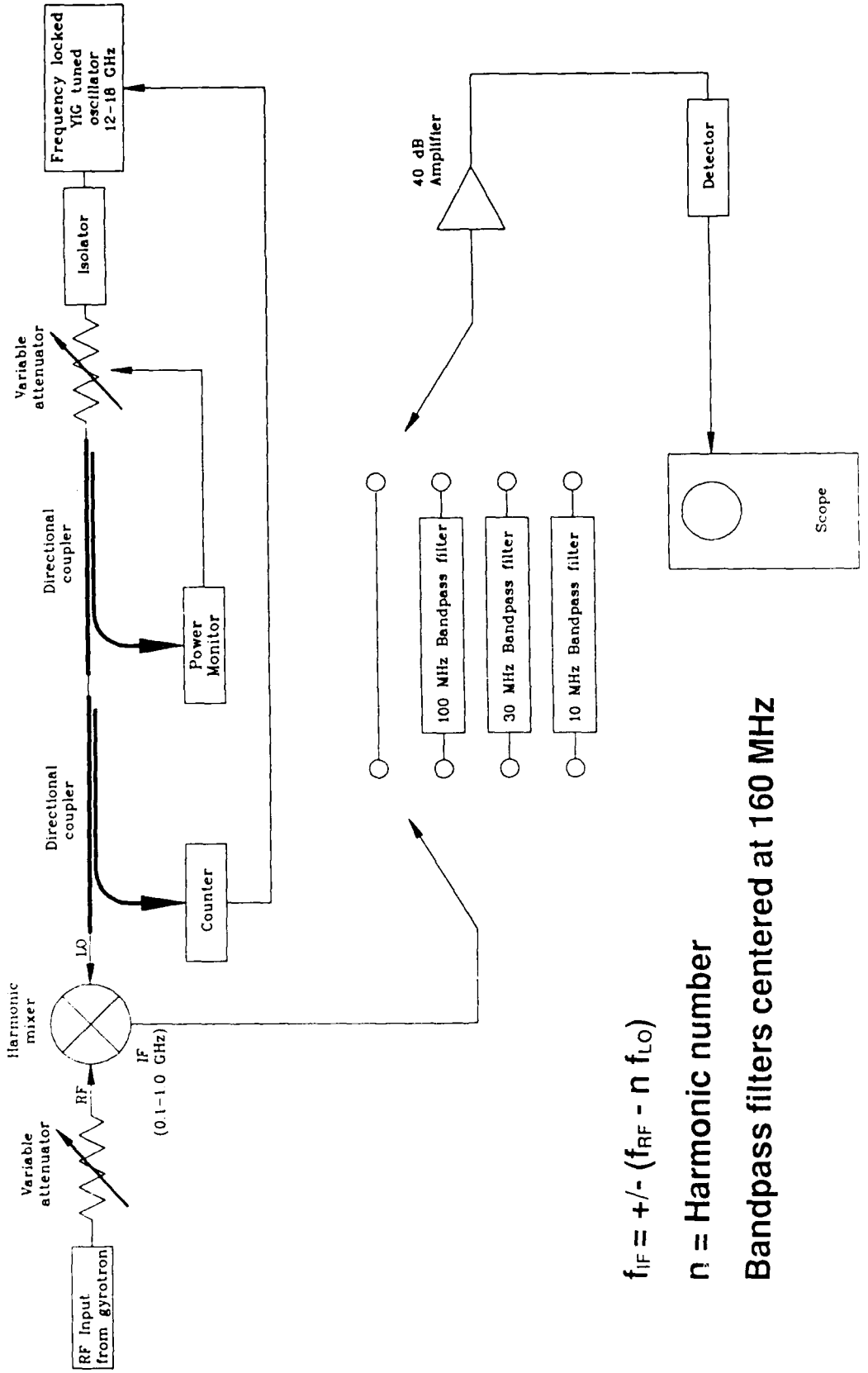

Fig. 9 — The heterodyne frequency diagnostic setup for the quasi-optical gyrotron

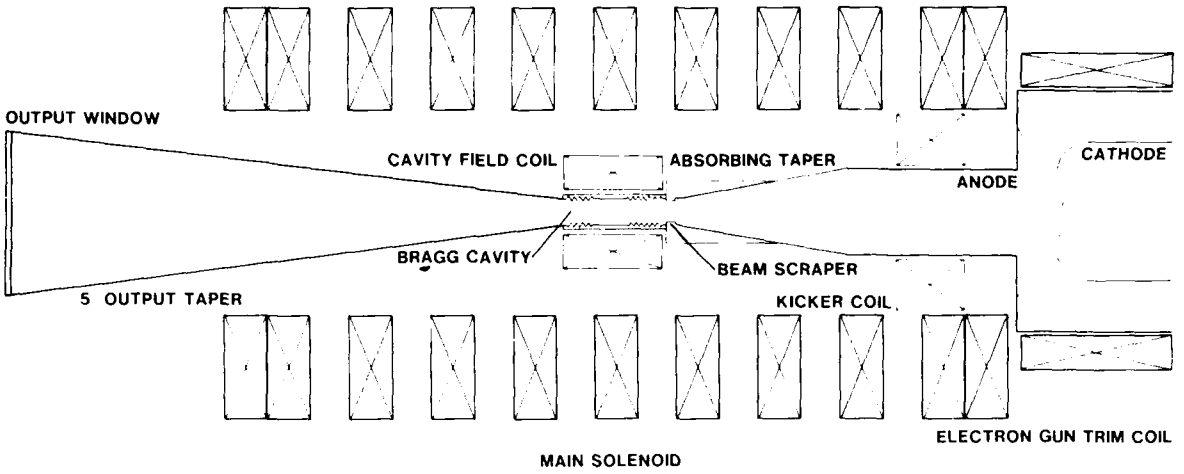

Fig. 10 — The NRL CARM

3.4 Small Period Wiggler FEL

The FEL operates by sending a high energy electron beam through a periodic magnetic field, the wiggler. If the periodicity of the wiggler is λ_w, then the wavelength of the radiation produced is given roughly by

$$\lambda = \lambda_w / 2\gamma^2. \tag{18}$$

Generally, a FEL is not a viable space-based source for beams with γ of 2 or 3, because the wiggler period is generally quite long—several centimeters at least. However, a potentially viable scheme for a space-based FEL would be one that used a very short wiggler period. The wiggler field falls off from the surface on which it is produced with scale length $\lambda_w/2\pi$. However, in a planar configuration, one could have the wiggler field strength fall off in the x direction, but extend very far in the y direction. (The beam propagates in the z direction.) Such a FEL could produce high power, but the electron beam would have to be a sheet beam rather than an annular beam (such as produced by a magnetron injection gun), or a pencil beam (such as produced by a Pierce gun). Like the CARM, the FEL demands a high-quality electron beam and has a wide instantaneous bandwidth. An experimental and theoretical program on small period wiggler FEL's exists at the University of Maryland [28]. There the hope is to build a three wiggler section klystron amplifier. The wiggler period is 4 mm and the beam voltage is 300 kV; the radiation will be at 1 mm wavelength and at a power of 100 kW. The inherent design efficiency is very small, less than 1%; however, with depressed collectors, it should be possible to raise this to 10% or more. Figure 11 shows a schematic of the U of Md short period wiggler FEL.

3.5 Summary

The development of sources to power a millimeter or submillimeter wavelength space-based radar is progressing rapidly. Much theoretical work has been done, and experiments are coming on-line to test the theoretical predictions. The sources described in subsections 3.1 to 3.4 are meant as examples only and are not meant as an exhaustive list. Other sources might be the orbitron [29,20] or gyro peniotron [31,32]. However, as apparent from the previous section, not only are source power and wavelength important, the phase must be coherent to a very high accuracy. Whether this

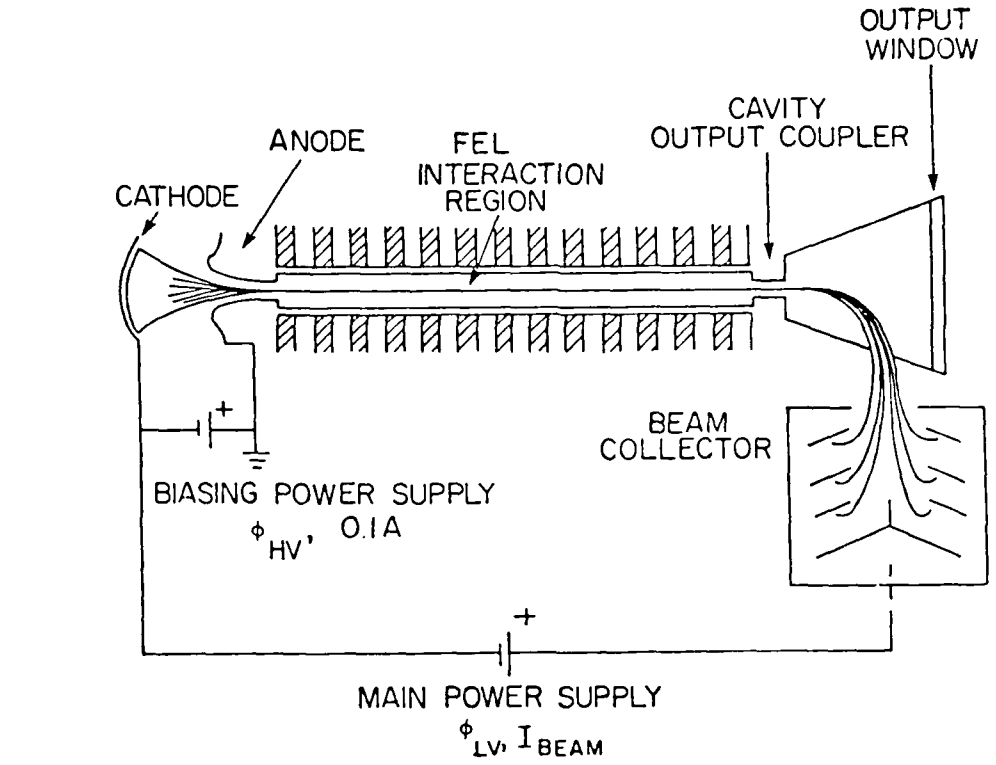

(a)

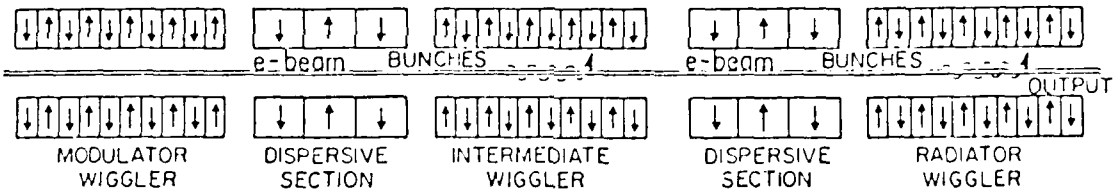

(b)

Fig. 11 — (a) The University of Maryland small period wiggler FEL and (b) the wiggler section for an amplifier configuration

is accomplished by an amplifier or a phase locked oscillator, it is important that this aspect of the research into rf sources not be overlooked.

ACKNOWLEDGMENT

The author thanks Richard Ford of the NRL Plasma Physics Division; Brooks Dodson, Stephen Mango, and Igor Jurkevich of the NRL Radar Division; and John McMahon of the NRL Optical Sciences Division for a number of very useful discussions, as well as Richard Temkim of MIT and Victor Granatstein of U of Md for pictures of their devices. This work was supported by the Office of Naval Research.

REFERENCES

1. M. Frerking, *Intl. J. Infrared and Millimeter Waves*, **8**, 1211, (1987).

2. G.N. Tsandoulas, *Science* **237**, 257 (1987).

3. J.F. Vesecky et al., Jason Technical Report JSR-80, Sept. 15, 1980.

4. N. Bloembergen and C.K. Patel, *Physics Today* **40**, 53 (1987).

5. N. Bloembergen and C.K. Patel, Report to the American Physical Society of the Study Group on Science and Technology of Directed Energy Weapons, American Physical Society, New York, p. 179; also *Rev. Mod. Phys.* **59**, 3, Part II (1987).

6. John J. Kovaly, ed., *Synthetic Aperture Radar* (Artech Publishing, Dedham, MA 1976).

7. T. Orzechowski et al., *Phys. Rev. Lett.* **57**, 2172 (1986).

8. L. Elias et al, *Phys. Rev. Lett.* **57**, 424 (1986).

9. V.A. Flyagin et al., 4th Intl. Symposium on Gyrotrons and FEL's; Bejing, China, June 1987.

10. K. Kreischer and R. Temkin, *Phys. Rev. Lett.* 59, 547 (1987).

11. S. Spira, K. Kreischer, and R. Temkin, Twelfth Intl. Conf. Infrared and Millimeter Waves, Orlando, FL, Dec. 1987, paper Th4.4, IEEE Cat87CH2490-1.

12. S. Gold et al., *Phys. Fluids* **30**, 2226 (1987).

13. M. Read, R. Seeley, and W. Manheimer, *IEEE Trans. Plasma Sci.* **PS**-13, 398 (1985).

14. A. McCurdy et al., *Phys. Rev. Lett.* **57**, 2379 (1986).

15. J. Burke et al., Twelfth Intl. Conf. Infrared and Millimeter Waves, 1987, paper T8.2.

16. P. Sprangle, J.Vomvoridis, and W. Manheimer, *Phys. Rev. A* **23**, 3127 (1981).

17. T. Hargreaves et al., *Int. J. Electron.* **57**, 997 (1984).

18. T. Hargreaves et al., Twelfth Intl. Conf. Infrared and Millimeter Waves, 1987, paper W8.1.

19. B. Levush and W. Manheimer, *Int. J. Infrared and Millimeter Waves*, **4**, 877 (1983).

20. B. Levush and W. Manheimer, *IEEE Trans. Wave Theory and Technologies* **32**, 1398 (1984).

21. A. Bondeson et al., *Int. J. Electron.* **53**, 547 (1982).

22. I.E. Botvinnik et al., *Sov. Tech. Phys. Lett.* **8**, 596 (1982).

23. A. Fliflet, *Int. J. Electron.* **61**, 1049 (1986).

24. A. Lin and C. Lin, *Int. J. Infrared and Millimeter Waves* **6**, 41 (1985).

25. R. McCowan et al., Twelfth Intl. Conf. Infrared and Millimeter Waves, 1987, paper Th8.4.

26. B. Danly, K. Pendergast, and R. Temkin, *Proc SPIE* **87** (1988).

27. A. Lin et al., Twelfth Intl. Conf. Infrared and Millimeter Waves, 1987, paper Th8.2.

28. J. Booske et al., Twelfth Intl. Conf. Infrared and Millimeter Waves, 1987, paper M8-5.

29. I. Alexeff and F. Dyer, *Phys. Rev. Lett.* **45**, 351 (1980).

30. J. Burke, W. Manheimer, and E. Ott, *Phys. Rev. Lett* **56**, 2625 (1986).

31. G. Dohler et al., *IEDM Technical Digest*, **845** (1984).

32. P. Vetiell, *IEEE Trans. Microwave Theory Tech.* **MTT-32**, 9917 (1984).

END

DATE

FILMED

8-88

DTIC